Supernovae and their host galaxies - V. The vertical distribution of supernovae in disc galaxies

A. A. Hakobyan, L. V. Barkhudaryan, A. G. Karapetyan, G. A. Mamon, D. Kunth, V. Adibekyan, L. S. Aramyan, A. R. Petrosian, M. Turatto

Monthly Notices of the ROYAL ASTRONOMICAL SOCIETY
MNRAS **471,** 1390–1400 (2017)
Advance Access publication 2017 June 26
doi:10.1093/mnras/stx1608

Supernovae and their host galaxies – V. The vertical distribution of supernovae in disc galaxies

A. A. Hakobyan,[1⋆] L. V. Barkhudaryan,[1] A. G. Karapetyan,[1] G. A. Mamon,[2] D. Kunth,[2] V. Adibekyan,[3] L. S. Aramyan,[1] A. R. Petrosian[1] and M. Turatto[4]

[1]Byurakan Astrophysical Observatory, 0213 Byurakan, Aragatsotn province, Armenia
[2]Institut d'Astrophysique de Paris, Sorbonne Universités, UPMC Univ Paris 6 et CNRS, UMR 7095, 98 bis bd Arago, F-75014 Paris, France
[3]Instituto de Astrofísica e Ciência do Espaço, Universidade do Porto, CAUP, Rua das Estrelas, P-4150-762 Porto, Portugal
[4]INAF – Osservatorio Astronomico di Padova, Vicolo dell'Osservatorio 5, I-35122 Padova, Italy

Accepted 2017 June 22. Received 2017 June 21; in original form 2017 April 21

ABSTRACT

We present an analysis of the height distributions of the different types of supernovae (SNe) from the plane of their host galaxies. We use a well-defined sample of 102 nearby SNe appearing inside high-inclined ($i \geq 85^\circ$), morphologically non-disturbed S0–Sd host galaxies from the Sloan Digital Sky Survey. For the first time, we show that in all the subsamples of spirals, the vertical distribution of core-collapse (CC) SNe is about twice closer to the plane of the host disc than the distribution of SNe Ia. In Sb–Sc hosts, the exponential scale height of CC SNe is consistent with those of the younger stellar population in the Milky Way (MW) thin disc, while the scale height of SNe Ia is consistent with those of the old population in the MW thick disc. We show that the ratio of scale lengths to scale heights of the distribution of CC SNe is consistent with those of the resolved young stars with ages from ∼10 up to ∼100 Myr in nearby edge-on galaxies and the unresolved stellar population of extragalactic thin discs. The corresponding ratio for SNe Ia is consistent with the same ratios of the two populations of resolved stars with ages from a few 100 Myr up to a few Gyr and from a few Gyr up to ∼10 Gyr, as well as with the unresolved population of the thick disc. These results can be explained considering the age–scale height relation of the distribution of stellar population and the mean age difference between Type Ia and CC SNe progenitors.

Key words: supernovae: general – Galaxy: disc – galaxies: spiral – galaxies: stellar content – galaxies: structure.

1 INTRODUCTION

The detailed understanding of the spatial distribution of supernovae (SNe) in galaxies provides a strong possibility to find the links between the nature of their progenitors and host stellar populations (e.g. van den Bergh 1997; Ivanov, Hamuy & Pinto 2000; Petrosian et al. 2005; Anderson & James 2008; Hakobyan et al. 2008, 2009; Kelly & Kirshner 2012; Nazaryan et al. 2013; Galbany et al. 2014; Taddia et al. 2015; Aramyan et al. 2016). Such studies allow us to constrain the important physical parameters of the different SN progenitors like their masses (e.g. Anderson et al. 2012; Kangas et al. 2017), ages (e.g. McMillan & Ciardullo 1996; Förster & Schawinski 2008) and metallicities (e.g. Modjaz et al. 2011; Galbany et al. 2016). For a comprehensive review addressing these issues, the reader is referred to Anderson et al. (2015).

According to the properties of SNe progenitors, they are divided into two general categories: core-collapse (CC) and Type Ia (thermonuclear) SNe. CC SNe are the colossal explosions that mark the violent deaths of young massive stars (e.g. Turatto 2003; Smartt 2009; Smith et al. 2011),[1] while SNe Ia are the explosive end in the evolution of binary stars in which one of the stars is an older white dwarf (WD) and the other star can be anything from a giant star to a WD (for a comprehensive review about thermonuclear SNe, see Maoz, Mannucci & Nelemans 2014). Type Ia SNe result from stars of different ages (from ∼0.5 up to ∼10 Gyr, see Maoz & Mannucci 2012) with a longer lifetime of progenitors than

⋆E-mail: hakobyan@bao.sci.am

[1] According to the spectral features in visible light, CC SNe are classified into three basic classes (e.g. Filippenko 1997): hydrogen lines are visible in the spectra of Type II SNe, but in Types Ib and Ic SNe; helium lines are seen in the spectra of SNe Ib, but in SNe Ic. Subclass IIn SNe are dominated by narrow emission lines, while subclass IIb SNe have transitional spectra closer to SNe II at early times, then evolving to SNe Ib.

Published by Oxford University Press on behalf of the Royal Astronomical Society

the progenitors of CC SNe (from a few Myr up to ∼0.2 Gyr when including the evolution of stars in close binary systems, see Zapartas et al. 2017).

Usually, the spatial distribution of SNe in S0–Sm galaxies is studied with the reasonable assumption that all CC SNe and the vast majority of SNe Ia belong to the disc, rather than the bulge population (e.g. van den Bergh 1997; Ivanov et al. 2000; Petrosian et al. 2005; Anderson & James 2008; Hakobyan 2008; Wang et al. 2013). Moreover, the distributions of SNe in the disc are studied assuming that the disc is infinitely thin (e.g. Hakobyan et al. 2009; Wang et al. 2013). The height distribution of SNe from the disc plane is mostly neglected while studying the host galaxies with low inclinations (close to face-on orientation) assuming that the exponential scale length of the radial distribution is dozens of times larger in comparison with the exponential scale height of SNe (e.g. Hatano, Branch & Deaton 1998).

Direct measurements of the heights of SNe and estimates of the scales of their vertical distributions in host galaxies with high inclination (close to edge-on orientation) were performed only in a small number of cases (McMillan 1997; Molloy 2012; Pavlyuk & Tsvetkov 2016). Mainly due to the small number statistics of SNe and inhomogeneous data of their host galaxies, the comparisons of vertical distributions of the different types of SNe resulted in statistically insignificant differences. Therefore, while the detailed study of the vertical distributions in edge-on galaxies has allowed to constrain ages, masses and other physical parameters of their components (e.g. Seth, Dalcanton & de Jong 2005; Yoachim & Dalcanton 2006; Bizyaev et al. 2014), the lack of analogous studies on the distribution of various SN types has prevented the determination of their parent populations via the direct comparison with the nearby extragalactic discs and the thick/thin discs of the Milky Way (MW) galaxy (e.g. Chen et al. 2001; Larsen & Humphreys 2003; Jurić et al. 2008).

The purpose of this paper is to address these questions properly through an investigation of the vertical distributions of the main classes of SNe in a nearby sample of 102 SNe and their well-defined edge-on S0–Sd host galaxies from the Sloan Digital Sky Survey-III (SDSS-III; Alam et al. 2015).

This is the fifth paper of the series and the content is as follows. Sample selection and reduction are introduced in Section 2. Section 3 describes the stellar disc model that we use to fit our data. All the results are discussed in Section 4. Section 5 summarizes our conclusions. To conform to values used in our data base (Hakobyan et al. 2012, hereafter Paper I), a cosmological model with $\Omega_{\rm m} = 0.27$, $\Omega_\Lambda = 0.73$ and $H_0 = 73\,{\rm km\,s^{-1}\,Mpc^{-1}}$ Hubble constant (Spergel et al. 2007) are adopted in this paper.

2 SAMPLE SELECTION AND REDUCTION

In this paper, we composed our sample by cross-matching the coordinates of classified Ia, Ibc[2] and II SNe from the Asiago Supernova Catalogue[3] (ASC; Barbon et al. 1999) with the footprint of SDSS Data Release 12 (DR12; Alam et al. 2015). All SNe are required to have equatorial coordinates. We use SDSS DR12 and the approaches are presented in Paper I to identify the host galaxies and classify their morphological types. It is worth noting that morphological classification of nearly edge-on galaxies is largely based on the visible size of the bulge relative to the disc because other morphological properties, such as the shape of spiral arms or presence of the bar, are generally obscured or invisible. The morphologies of galaxies are restricted to S0–Sd types since we are interested in studying the vertical distribution of SNe in host stellar discs. A small number of Sdm–Sm host galaxies are not selected because they show no clear discs.

From the signs of galaxy–galaxy interactions, we classify the morphological disturbances of the hosts in the SDSS DR12 by following the techniques described in detail in Hakobyan et al. (2014, hereafter Paper II). We then exclude from this analysis any galaxy disc exhibiting strong disturbances: interacting, merging and post-merging/remnant.

Using the techniques presented in Paper I, we measure the apparent magnitudes and the geometry of host galaxies.[4] In the SDSS g-band, we first construct isophotes and then centre at the each galaxy centroid position an elliptical aperture visually fitted to the 25 mag arcsec^{-2} isophote. We measure the apparent magnitudes, major axes (D_{25}), position angles (PA) of the major axes and elongations (a/b) of galaxies using these apertures. In this analysis, we correct the magnitudes and D_{25} for the Galactic and host galaxy internal extinction (see Paper I).

2.1 Inclination

The main difficulty in measuring the vertical distribution of SNe above the host stellar discs is that we have no way of knowing where along the line of sight the SNe lie. This means that reliable measurements can only be done in discs that are highly inclined, i.e. closer to an edge-on orientation (e.g. $85^\circ \le i \le 90^\circ$). In contrast to galaxies with a lower inclination, the matter is complicated by the difficulty of making an accurate determination of the inclination angle. For these galaxies, the inclination cannot be measured simply from the major and minor axes because the presence of a central bulge places a limit on the axial ratio even for a perfectly edge-on galaxy.

This problem with the bulge has been solved by using the axial ratio of the exponential disc that fits in the g-band provided by the SDSS (from the model with an $r^{1/4}$ bulge and exponential disc), i.e. `expAB_g`. Indeed, real stellar discs are not flat with negligible thicknesses, but have some intrinsic width, and a proper measurement of the inclination depends on this intrinsic ratio of the vertical and horizontal axes of the disc, known as q. Therefore, we calculate the inclinations of SNe host galaxies following the formula

$$\cos^2 i = \frac{(\texttt{expAB\_g})^2 - q^2}{1 - q^2}, \qquad (1)$$

where i is the inclination angle in degrees between the polar axis and the line of sight and q is the intrinsic axial ratio of viewed edge-on galaxies. According to Paturel et al. (1997),

$$q = {\rm dex}[-(0.43 + 0.053\,t)] \qquad (2)$$

for $-1 \le t \le 7$, where t is the morphological type code. Using equations (1) and (2), we restrict the inclinations of host galaxies to $85^\circ \le i \le 90^\circ$.

[2] ‘Stripped-envelope’ SNe of Types Ib and Ic, including the mixed Ib/c with uncertain subclassification, are denoted as SNe Ibc.

[3] We use the updated version of the catalogue, which includes all classified SNe exploded before 2015 January 1.

[4] Instead of using the data from Paper I, which is based on the SDSS DR8, for homogeneity, we re/measure the magnitudes and the geometry of all host galaxies, with additional new SN hosts included, based only on DR12.

Table 1. Numbers of SNe as a function of morphological types of edge-on S0–Sd host galaxies.

	S0	S0/a	Sa	Sab	Sb	Sbc	Sc	Scd	Sd	All
Ia	6	3	2	5	9	5	16	4	3	53
Ibc	0	0	0	0	2	0	1	3	3	9
II	0	1	1	1	11	6	12	5	3	40
All	6	4	3	6	22	11	29	12	9	102

Notes. Among SNe II, four are of Type IIb (two in Sb and two in Scd galaxies). Due to the uncertainties in the progenitor nature of Type IIn SNe, and often their misclassification (e.g. Anderson et al. 2012; Habergham et al. 2014), we remove them from the sample.

All the selected SNe host galaxies are visually inspected because sometimes bright stars projected nearby, strong dust layers, bright nuclear/bulge emission, large angular sizes, etc. do not allow the SDSS automatic algorithm to correctly determine the parameters of galaxies, in particular the axial ratio expAB_g. The host discs with a clearly seen dust layer, or without signs of non-edge-on spiral arms, are selected as true edge-on galaxies. In other words, we exclude the discs whose galactic plane is not aligned along the major axis of their fitted elliptical apertures (e.g. warped edge-on discs, see Reshetnikov et al. 2016). As a result, we select 106 SNe in edge-on host galaxies.

In S0–Sd galaxies, all CC SNe and the vast majority of Type Ia SNe belong to the disc, rather than the bulge component (Hakobyan et al. 2016, hereafter Paper III). Therefore, for the selected 106 SNe in this restricted sample of edge-on galaxies, we perform a visual inspection of the SNe positions on the SDSS images to identify the SNe from the bulge population of host galaxies. The result is that three Type Ia (1990G, 1993aj and 2003ge) and one Type Ib/c (2005E) SNe may belong to the bulge because of their location. The three SNe Ia are clearly outside the host discs, located far in the bulge population. The Type Ib/c SN is also located far from the host galaxy disc but it is a peculiar, calcium-rich SN whose nature is still under debate and may have a different progenitor from the typical CC (e.g. Perets et al. 2010). All these four SNe are excluded from the sample.

After these restrictions, we are left with a sample of 102 SNe within 100 host galaxies. The mean distance of this sample is 100 ± 8 Mpc, and the median distance and standard deviation are 78 and 84 Mpc, respectively. The mean D_{25} of our host galaxies is 108 ± 10 arcsec with the smallest value of 22 arcsec. Table 1 displays the distribution of all SNe types among the various considered morphological types of host galaxies. Fig. 1 shows images of typical examples of edge-on host galaxies with marked positions of SNe.

2.2 Measurements of the heights of SNe

The heights of SNe above the host galactic plane might be calculated by using the simple formulas presented in Hakobyan et al. (2009) with available SNe offsets from host galaxy nuclei and PA of the galaxies (also see Paper III). However, as demonstrated in Paper I, SN catalogues report different offsets with different levels of accuracy. Individual offsets are based on the determination of the positions of the host galaxy nuclei, which might be uncertain and depend on many factors (e.g. colour of the image, plate saturation, galaxy peculiarity, incorrect SDSS fibre targeting of the galaxy nucleus, etc.). For more details, the reader is referred to Paper I.

For this study, using the SN coordinates and its edge-on host galaxy image in the SDSS g-band, we measure the perpendicular distance, i.e. the height, from the major axis of the fitted elliptical aperture of each galaxy to the position of SN. At the same time, using the coordinates of the host galaxy nucleus, we also measure the projected galactocentric radius of the SN along the same major axis.[5] Fig. 2 schematically illustrates the geometrical location of an SN within an edge-on disc, where $\textsc{v}$ is the height (in arcsec) and $\textsc{u}$ is the projected galactocentric radius (in arcsec) of the SN. A similar technique was also used in Pavlyuk & Tsvetkov (2016) on the Digital Sky Survey (DSS) images to determine the $\textsc{v}$ and $\textsc{u}$ coordinates of SNe.

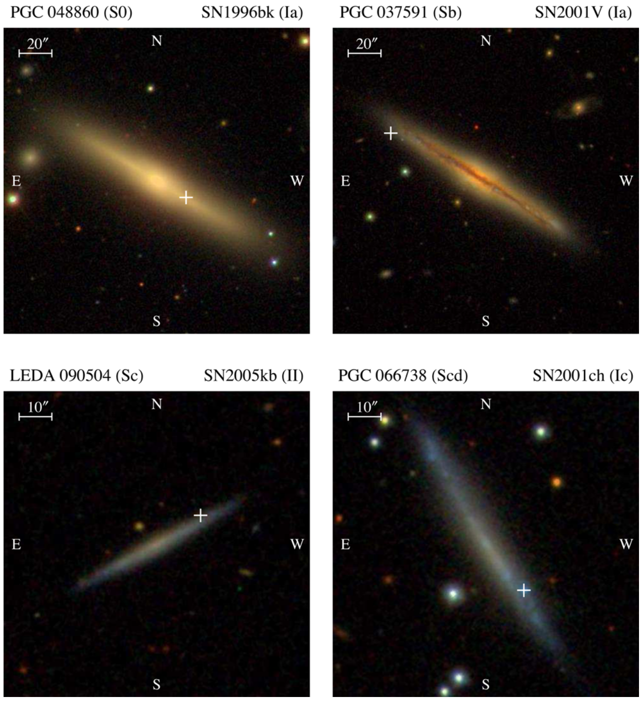

Figure 1. SDSS images representing examples of edge-on SNe host galaxies. The objects' identifiers with host morphologies and SN types (in parentheses) are listed at the top. The positions of SNe (marked by a cross sign) are also shown. In all images, north is up and east to the left.

It is important to note that, as in the case of the radial distribution of SNe in face-on galaxies (Hakobyan et al. 2009), the distribution of linear distances in the vertical direction is biased by the greatly different intrinsic sizes of host discs. Fig. 3 illustrates the comparison of the heights $\textsc{v}$ of SNe and R_{25} of host galaxies in kpc. Also shown are the best-fitting lines

$$\log(\textsc{v}_{\rm Ia}) = (-1.10 \pm 0.11) + (0.89 \pm 0.08)\ \log(R_{25}) \text{ and}$$

$$\log(\textsc{v}_{\rm CC}) = (-1.68 \pm 0.15) + (1.07 \pm 0.13)\ \log(R_{25})$$

with near unity slopes. To check the significance of the correlations, we use the Spearman's rank correlation test, which indicates a strong positive trend between the heights and R_{25} for Type Ia SNe ($r_s = 0.382$, $P = 0.005$), while not significant for CC SNe ($r_s = 0.166$, $P = 0.255$). Therefore, in the remainder of this study, we use only relative heights and projected galactocentric radii of SNe, i.e. normalized to $R_{25} = D_{25}/2$ of host galaxies in the g-band.

[5] We remind that in comparison with the measured heights, the measurements of projected galactocentric radii of SNe include some minor inaccuracy because of the mentioned uncertain determination of the exact point like positions of host galaxy nuclei. The projected galactocentric radii are only used in Fig. 5 of Section 4.1 for ancillary purposes.

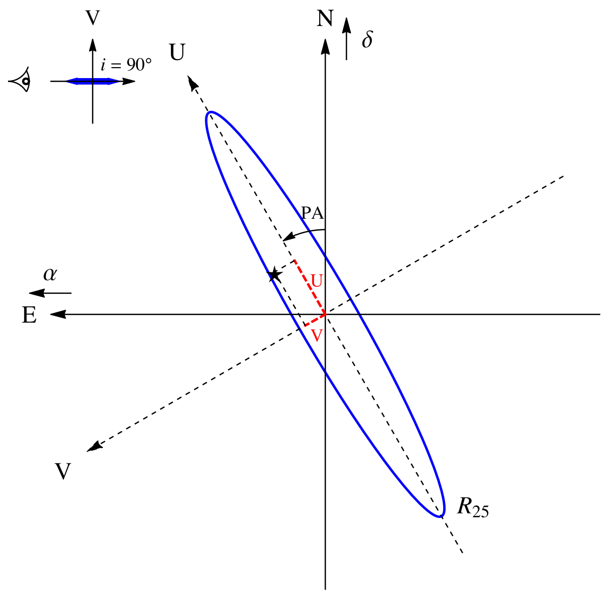

Figure 2. Location of the SN within its edge-on host galaxy. The centre of the galaxy is at the origin of coordinate systems and the asterisk is the projected location of the SN. The U (the projected galactocentric radius) and V (the height) are coordinates of the SN in the host galaxy coordinate system along the major (U) and minor (V) axes, respectively. The inset in the upper-left corner illustrates the 90° inclination of the polar axis of the galaxy with respect to the line of sight.

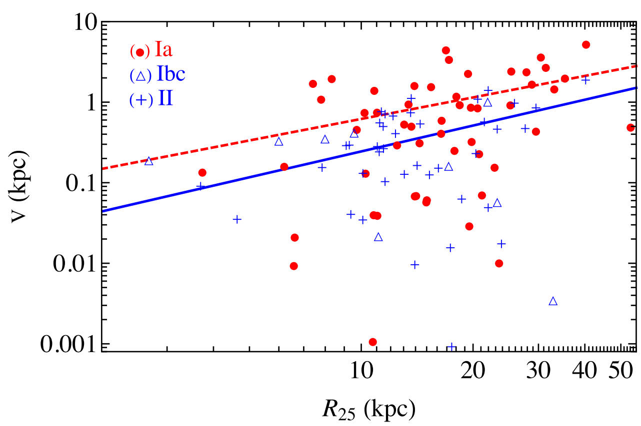

Figure 3. Comparison of the heights v of SNe and R_{25} of host galaxies in kpc. Red circles, blue triangles and crosses, respectively, show Types Ia, Ibc and II SNe. Red dashed (Ia) and blue solid (Ibc+II) lines are best fits to the samples.

The full data base of 102 individual SNe (SN designation, type, equatorial coordinates, V and U) and their 100 host galaxies (galaxy SDSS designation, distance, morphological type and corrected g-band D_{25}) is available in the online version (Supporting Information) of this paper.

3 THE MODEL OF STELLAR DISC

In our model, the volumetric density $\rho^{\rm SN}(\tilde{r}, \tilde{z})$ of SNe in the host axisymmetric stellar discs is assumed to vary as follows in the radial $\tilde{r}$ and vertical $\tilde{z}$ directions:

$$\rho^{\rm SN}(\tilde{r}, \tilde{z}) = \rho_0^{\rm SN} \exp(-\tilde{r}/\tilde{h}_{\rm SN}) f(\tilde{z}) \, , \qquad (3)$$

where $\tilde{r} = R_{\rm SN}/R_{25}$, $\tilde{z} = z_{\rm SN}/R_{25}$ and $(R_{\rm SN}, z_{\rm SN} \equiv {\rm v})$ are cylindrical coordinates, $\rho_0^{\rm SN}$ is the central volumetric density, $\tilde{h}_{\rm SN} = h_{\rm SN}/R_{25}$ is the radial scale length and $f(\tilde{z})$ is a function describing the vertical distribution of SNe.

In equation (3), we adopt a generalized vertical distribution

$$f(\tilde{z}) = {\rm sech}^{2/n} \left(n\tilde{z}/\tilde{z}_0^{\rm SN}\right) , \qquad (4)$$

where $\tilde{z}_0^{\rm SN} = z_0^{\rm SN}/R_{25}$ is the vertical scale height of SNe and n is a parameter controlling the shape of the profile near the plane of the host galaxy. Following the vertical surface brightness distribution of edge-on galaxies (e.g. de Grijs, Peletier & van der Kruit 1997; Bizyaev & Mitronova 2002), we also assume that the scale height of SNe is independent of the projected galactocentric radius (see also de Grijs & Peletier 1997, for late-type galaxies), i.e. there is no disc flaring.

Recent photometric fits to the surface brightness distribution of a large number of edge-on galaxies in near-infrared (Mosenkov, Sotnikova & Reshetnikov 2010) and SDSS g-, r- and i-bands (Bizyaev et al. 2014, see also Yoachim & Dalcanton 2006 for other photometric bands) suggest that a value of $n = 1$ is an appropriate model of stellar discs. When $n \rightarrow \infty$, Equation (4) reduces to $f(\tilde{z}) \sim \exp(-|\tilde{z}|/\tilde{H}_{\rm SN})$, where $\tilde{H}_{\rm SN} = \tilde{z}_0^{\rm SN}/2$ at large heights, and is widely used to successfully fit the dust distribution in edge-on galaxies (e.g. Bianchi 2007; Bizyaev et al. 2014).

In linear units, the exponential (exp) form of $f(\tilde{z})$ is used to model the distribution of Galactic stars (e.g. Chen et al. 2001; Larsen & Humphreys 2003), novae (e.g. Hatano et al. 1997a), SNe (e.g. Dawson & Johnson 1994; Hatano, Fisher & Branch 1997b), SN remnants (e.g. Ilovaisky & Lequeux 1972), pulsars (e.g. Andreasyan, Andreasyan & Paronyan 2016) and extragalactic SNe (e.g. McMillan 1997; Hatano et al. 1998; Pavlyuk & Tsvetkov 2016), while the sech^2 form is used to fit the vertical distribution of resolved stars (Seth et al. 2005) and CC SNe (Molloy 2012) in highly inclined nearby galaxies.

Note that sech^2 profile ($n = 1$) is expected for an isothermal stellar population (Spitzer 1942), while exp profile ($n \rightarrow \infty$) can be obtained by a combination of isothermal stellar populations with different 'temperatures' (velocity dispersions). At large heights, ${\rm sech}^2(x) \rightarrow 4\exp(-2x)$, and at low heights, the sech^2 profile is uniform, while the exp profile is cuspy.

4 RESULTS AND DISCUSSION

4.1 The vertical distribution and scale height of SNe

We fit sech^2 and exp forms of $f(\tilde{z})$ profile to the distribution of normalized absolute heights ($|\tilde{z}| \equiv |{\rm v}|/R_{25}$) of SNe using the maximum likelihood estimation (MLE) method. Here, because of the small number statistics of Type Ibc SNe (see Table 1), we group them with Type II SNe in a larger CC SNe sample. Fig. 4 shows the histograms of the normalized heights with the fitted sech^2 and exp probability density functions (PDFs) for Type Ia and CC SNe in Sa–Sd galaxies.[6] In columns 4, 7 and 10 of Table 2, we list the mean values of $|\tilde{z}|$ and the maximum likelihood scale heights for both types of SNe in various subsamples of host galaxies.

[6] For this comparative illustration, we do not include S0–S0/a galaxies because they host almost only Type Ia SNe (see Table 1). For the sake of visualization, the distribution of Type Ibc SNe is also presented in the bottom panel of Fig. 4.

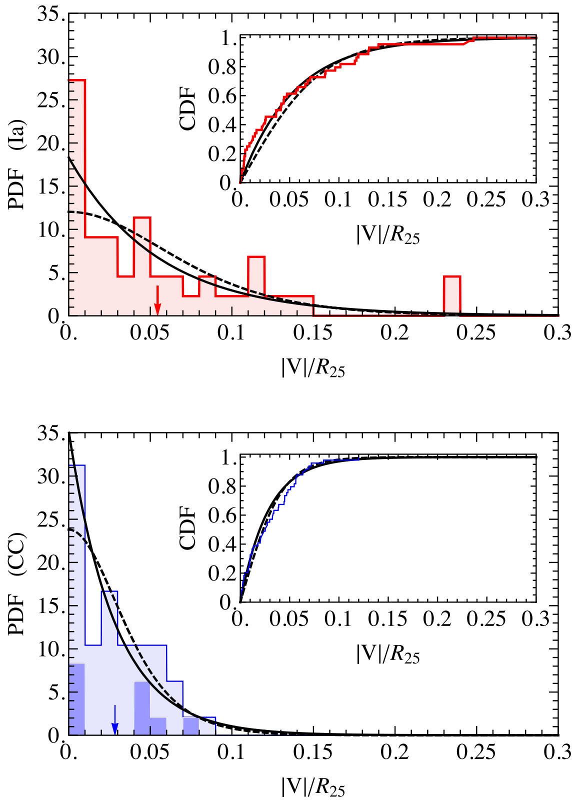

Figure 4. Vertical distribution of SNe (scaled to the isophotal radius of the disc) in Sa–Sd galaxies. Upper panel: fitted sech^2 (dashed curve) and exp (solid curve) PDFs of the normalized absolute heights ($|\tilde{z}| \equiv |\mathrm{v}|/R_{25}$) of Type Ia SNe (red histogram). Bottom panel: the same for CC SNe (blue histogram). The dark blue histogram presents the distribution of Type Ibc SNe only. The insets present the different forms of fitted CDFs in comparison with the SN distribution. The mean values of the distributions are shown by arrows.

From column 4 of Table 2, it immediately becomes clear that in all the subsamples of host galaxies the vertical distribution of CC SNe is about twice closer to the plane of the host disc than the distribution of Type Ia SNe. In fact, the two-sample Kolmogorov–Smirnov (KS) and Anderson–Darling (AD) tests,[7] shown in Table 3, indicate that this difference is statistically significant in Sa–Sd galaxies, although not significant if only late-type hosts are considered.

Note that four Type IIb SNe are included in Type II SNe sample (see Table 1). For Sa–Sd galaxies, it also might be reasonable to group Types IIb and Ibc SNe as a wider ‘stripped-envelope’ (SE) SN class (13 objects) and compare them with pure Type II SNe (35 objects). However, we find no difference between the vertical distributions of SE and pure Type II SNe ($P_{\mathrm{KS}} = 0.401$, $P_{\mathrm{AD}} = 0.320$), resulting in statistically indistinguishable scale lengths between these SN types. Therefore, in the remainder of this study, we will group all these subtypes as the main CC SN sample and compare that with the Type Ia SN sample.

[7] The two-sample AD test is more powerful than the KS test (Engmann & Cousineau 2011), being more sensitive to differences in the tails of distributions. Traditionally, we chose the threshold of 5 per cent for significance levels of the different tests.

It is important to note that the dust extinction in edge-on SN host galaxies might have an impact on our estimated scale heights.[8] In Paper I, we demonstrated that in general there is a lack of SNe host galaxies with high inclinations, which can be explained by a bias in the discovery of SNe due to strong dust extinction (e.g. Cappellaro & Turatto 1997), particularly in edge-on hosts (e.g. Holwerda et al. 2015).

The vertical distribution of dust in disc galaxies has an exponential profile with about three times smaller scale height in comparison with the distribution of all stars ($H_{\mathrm{stars}}/H_{\mathrm{dust}} \approx 3$, e.g. Bianchi 2007).[9] Analysing the vertical distribution of the resolved stellar populations in nearby edge-on galaxies, Seth et al. (2005) found that the dust has a negligible impact on the distribution parameters of stars at $|z| \gtrsim H_{\mathrm{dust}}$ heights (for the edge-on surface brightness profiles of unresolved populations, see e.g. Bianchi 2007). Therefore, in Table 2, to check the impact of the dust extinction on the obtained scale heights, we also estimate the distribution parameters considering the SNe in Sa–Sd galaxies only at $|\tilde{z}| > \tilde{H}_{\mathrm{dust}}$ heights. For the average dust scale height, we use $\tilde{H}_{\mathrm{dust}} = 0.02$, roughly considering that $H_{\mathrm{dust}} \approx H_{\mathrm{Ia}}/3$ (see also Della Valle & Panagia 1992). In Fig. 5, we show the distribution of coordinates of SNe along the major (u/R_{25}) and minor axes ($\tilde{z} \equiv \mathrm{v}/R_{25}$) of their Sa–Sd host galaxies with the $|\tilde{z}| \leq 0.02$ opaque region, and for the sake of visualization, we scale the distribution to the PGC 037591 galaxy (also shown in Fig. 1, better known as NGC 3987), which is one of the representatives of the edge-on galaxies with a prominent dust line along the major axis.

From columns 7 and 10 of Table 2 (the subsamples of Sa–Sd hosts labelled with ‘†’ symbols), despite the small number statistics (column 3), we see that the extinction by dust near to the plane of host galaxies does not strongly bias the estimated scale heights of SNe. The scale height of CC SNe with $|\tilde{z}| > 0.02$ is almost equal to that with the $|\tilde{z}| \geq 0$, while the scale height of Type Ia SNe with $|\tilde{z}| > 0.02$ is only ∼15 per cent greater (still statistically insignificant) than that with the $|\tilde{z}| \geq 0$. In the remainder of this study, we will generally use the scale heights of SNe without height-truncation due to the small number statistics and insignificance of the effect, however, if needed, we will emphasize the impact of the dust extinction on the scale heights.

To check whether the distribution of SN heights follows the best-fitting profiles, we perform one-sample KS and AD tests on the cumulative distribution of the normalized absolute heights ($|\tilde{z}|$), where the sech^2 and exp models have $E(|\tilde{z}|) = \tanh(|\tilde{z}|/\tilde{z}_0^{\mathrm{SN}})$ and $E(|\tilde{z}|) = 1 - \exp(-|\tilde{z}|/\tilde{h}_{\mathrm{z}}^{\mathrm{SN}})$ cumulative distribution functions (CDFs), respectively. Columns 5, 6, 8 and 9 of Table 2 show the KS and AD probabilities that the vertical distributions are drawn from the best-fitting profile. Cumulative distributions of the heights and CDFs of the fitted forms for Type Ia and CC SNe in Sa–Sd galaxies are presented in the insets of Fig. 4.

From columns 5, 6, 8 and 9 of Table 2, we see that the vertical distribution is consistent with both profiles in most subsamples of Type Ia SNe and in all subsamples of CC SNe. For Type Ia

[8] Another factor, such as a deviation from the perfectly edge-on orientation of the host discs, may also affect our estimation of the scale heights, increasing them. However, we are quite confident that our galaxies can vary by a few degrees only from the perfectly edge-on orientation (see Section 2.1). In addition, other authors have demonstrated that slight deviations from $i = 90°$ have minimal impact on the derived structural parameters of the vertical distributions of different stellar populations (e.g. de Grijs et al. 1997).

[9] This value can vary from two to four, depending, respectively, on early- and late-type morphology of edge-on spiral galaxies (e.g. De Geyter et al. 2014).

Table 2. Consistency and scale heights of the vertical distributions of Type Ia and CC SNe in edge-on galaxies with sech^2 ($n = 1$) and exp ($n \to \infty$) models.

					$n = 1$			$n \to \infty$	
Host (1)	SN (2)	$N_{\rm SN}$ (3)	$\langle\lvert\tilde{z}\rvert\rangle$ (4)	$P_{\rm KS}$ (5)	$P_{\rm AD}$ (6)	$\tilde{z}_0^{\rm SN}$ (7)	$P_{\rm KS}$ (8)	$P_{\rm AD}$ (9)	$\tilde{H}_{\rm SN}$ (10)
S0–Sd	Ia	53	0.058 ± 0.009	0.068	**0.012**	0.089 ± 0.015	0.196	0.165	0.058 ± 0.009
Sa–Sd	Ia	44	0.055 ± 0.009	0.147	**0.031**	0.083 ± 0.012	0.319	0.239	0.055 ± 0.007
Sa–Sd	CC	48	0.028 ± 0.003	0.644	0.209	0.042 ± 0.004	0.648	0.287	0.028 ± 0.003
Sa–Sd†	Ia	28	0.082 ± 0.011	0.983	0.973	0.098 ± 0.014	0.970	0.973	0.062 ± 0.012
Sa–Sd†	CC	28	0.044 ± 0.003	0.459	0.723	0.041 ± 0.006	0.331	0.525	0.024 ± 0.004
Sa–Sbc	Ia	21	0.061 ± 0.014	0.168	0.055	0.094 ± 0.014	0.371	0.151	0.061 ± 0.011
Sa–Sbc	CC	21	0.028 ± 0.004	0.860	0.299	0.040 ± 0.005	0.492	0.239	0.028 ± 0.003
Sc–Sd	Ia	23	0.049 ± 0.011	0.627	0.354	0.073 ± 0.018	0.849	0.919	0.049 ± 0.009
Sc–Sd	CC	27	0.029 ± 0.005	0.493	0.353	0.044 ± 0.007	0.497	0.684	0.029 ± 0.004
Sb–Sc	Ia	30	0.064 ± 0.011	0.476	0.212	0.096 ± 0.016	0.679	0.482	0.065 ± 0.012
Sb–Sc	CC	32	0.028 ± 0.004	0.476	0.203	0.042 ± 0.007	0.586	0.264	0.028 ± 0.003
Sb–Sc†	Ia	21	0.089 ± 0.013	0.853	0.962	0.108 ± 0.021	0.594	0.821	0.070 ± 0.014
Sb–Sc†	CC	19	0.044 ± 0.004	0.908	0.948	0.041 ± 0.008	0.728	0.794	0.024 ± 0.006
Sb–Sc*	Ia	24	0.065 ± 0.014	0.686	0.281	0.097 ± 0.020	0.927	0.657	0.065 ± 0.014
Sb–Sc*	CC	31	0.028 ± 0.004	0.422	0.224	0.042 ± 0.007	0.576	0.335	0.028 ± 0.004

Notes. Columns 1 and 2 give the subsample; Column 3 is the number of SNe in the subsample; Column 4 is the mean of the normalized absolute vertical distribution with the error of the mean; Columns 5 and 6 are the $P_{\rm KS}$ and $P_{\rm AD}$ probabilities from one-sample KS and AD tests, respectively, that the vertical distribution of SNe is drawn from the best-fitting sech^2 profile; Column 7 is the maximum likelihood value of the scale height with a bootstrapped error (repeated 10^3 times); Columns 8, 9 and 10 are, respectively, the same as Columns 5, 6 and 7, but for the best-fitting exp profile. The subsamples labelled with '†' symbols correspond to SNe with $|\tilde{z}| > 0.02$. The subsamples labelled with '*' symbols correspond to SNe with distances ≤200 Mpc. We calculate the $P_{\rm KS}$ and $P_{\rm AD}$ using the calibrations by Massey (1951) and D'Agostino & Stephens (1986), respectively. The statistically significant deviations from the best-fitting profile are highlighted in bold.

Table 3. Comparison of the normalized absolute vertical distributions ($|\tilde{z}| \equiv |{\rm v}|/R_{25}$) of SNe amongst different pairs of subsamples.

Subsample 1				Subsample 2				
Host	SN	$N_{\rm SN}$		Host	SN	$N_{\rm SN}$	$P_{\rm KS}$	$P_{\rm AD}$
Sa–Sd	Ia	44	versus	Sa–Sd	CC	48	**0.045**	**0.025**
Sa–Sd†	Ia	28	versus	Sa–Sd†	CC	28	**0.011**	**0.003**
Sa–Sbc	Ia	21	versus	Sa–Sbc	CC	21	**0.041**	**0.037**
Sc–Sd	Ia	23	versus	Sc–Sd	CC	27	0.690	0.310
Sa–Sbc	Ia	21	versus	Sc–Sd	Ia	23	0.387	0.440
Sa–Sbc	CC	21	versus	Sc–Sd	CC	27	0.765	0.802
Sb–Sc	Ia	30	versus	Sb–Sc	CC	32	**0.039**	**0.009**
Sb–Sc†	Ia	21	versus	Sb–Sc†	CC	19	**0.013**	**0.001**
Sb–Sc*	Ia	24	versus	Sb–Sc*	CC	31	0.112	**0.028**

Notes. The subsamples labelled with '†' symbols correspond to SNe with $|\tilde{z}| > 0.02$. The subsamples labelled with '*' symbols correspond to SNe with distances ≤200 Mpc. The $P_{\rm KS}$ and $P_{\rm AD}$ are the probabilities from two-sample KS and AD tests, respectively, that the two distributions being compared are drawn from the same parent distribution. The $P_{\rm KS}$ and $P_{\rm AD}$ are calculated using the calibrations by Massey (1951) and Pettitt (1976), respectively. The statistically significant differences between the distributions are highlighted in bold.

SNe in Sa–Sd (also in S0–Sd) galaxies, the vertical distribution is consistent with the exp profile, but not with the sech^2 one (as seen in the AD statistic but only very marginally in the KS statistic). When we separate SNe Ia between early- and late-type host galaxies, the inconsistency vanishes with only barely AD test significance in early-type spirals (see the $P_{\rm AD}$ value in column 6 of Table 2 for SNe Ia in Sa–Sbc galaxies). The $\langle|\tilde{z}|\rangle$ value (scale heights too) for SNe Ia is ∼25 per cent greater in Sa–Sbc galaxies than that in Sc–Sd hosts (although the difference is not significant, see Table 3), while for CC SNe this parameter has a nearly constant value in the mentioned subsamples. This effect can be attributed to the earlier and wider morphological distribution of SNe Ia host galaxies (from S0/Sa to Sd, see Table 1 and also Papers I and II) in comparison with CC SNe hosts, and the systematically thinner vertical distribution of the host stellar population from early- to late-type discs (e.g. de Grijs 1998; Yoachim & Dalcanton 2006; Bizyaev et al. 2014).

In the first attempts to estimate the mean value of the vertical coordinates of SNe, Tsvetkov (1981, 1987) used the distribution of SN colour excesses without precise information on their spectroscopic types and host galaxy morphology in a sample of non-edge-on spirals. No difference was found in the vertical distributions of Type I and II SNe with an indication that both types belong to the young Population I. However, the inclinations of host galaxies and the uncertain separation[10] of SN types might be the reason for the similarity between the vertical distributions of the mentioned SN types. Using similar colour excess data of the best photometrically studied Type Ia SNe in late-type galaxies, Della Valle & Panagia (1992) showed that these SNe have a considerably broader vertical distribution than the dust discs of their hosts and concluded that SNe Ia are older than the old disc population.

Direct measurements of the heights of SNe and estimation of the scales of their vertical distributions were performed only in a small number of cases (McMillan 1997; Molloy 2012; Pavlyuk & Tsvetkov 2016). McMillan (1997) examined the offsets between the major axes of a sample of highly inclined ($i \geq 60°$) galaxies and the SNe they hosted in an attempt to measure the scale heights of Type Ia and II SNe. Unfortunately, the sample of such objects was quite small (66 galaxies), especially when restricted to

[10] Type Ibc SNe were labelled as 'I pec' types during observations before 1986 and included in the sample of Type I SNe.

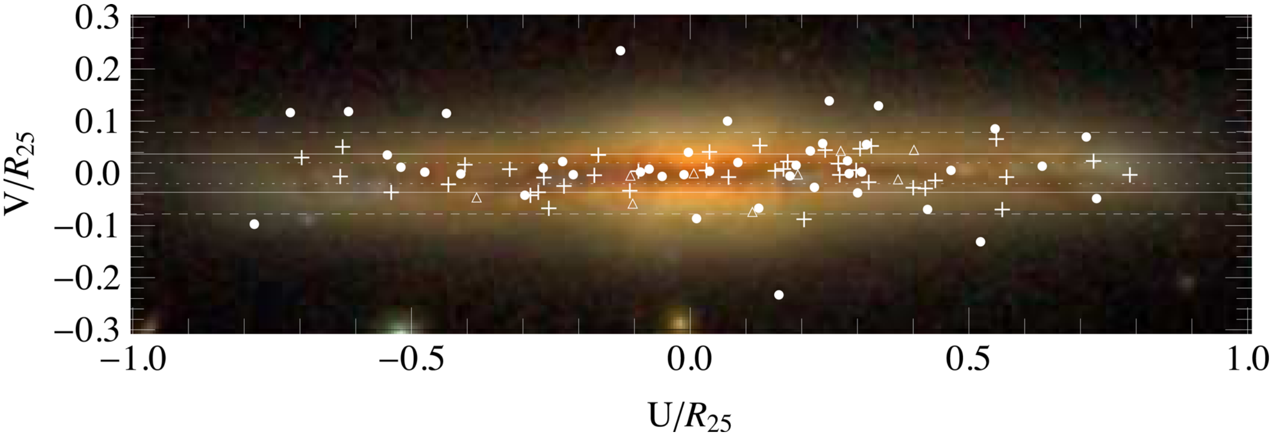

Figure 5. Distribution of coordinates of SNe along the major (U/R_{25}) and minor axes ($\tilde{z} \equiv$ V/R_{25}) of their Sa–Sd host galaxies. Circles, triangles and crosses, respectively, show Types Ia, Ibc and II SNe. 1σ intervals of the distributions of the $\tilde{z}$ coordinates for Type Ia and CC (Ibc+II) SNe are presented by dashed ($\sigma = 0.078$) and solid ($\sigma = 0.037$) lines, respectively. The background SDSS image shows the PGC 037591 galaxy (scaled to the distribution), which is one of the representatives of the edge-on galaxies with a prominent dust line along the major axis. Dotted lines show the $|\tilde{z}| \leq 0.02$ opaque region.

galaxies at $i \geq 75°$, which resulted in statistically indistinguishable vertical distributions (in kpc) between the mentioned types of SNe. Molloy (2012) used data from the ASC to study the vertical distribution (in kpc) of 64 CC SNe in highly inclined ($i \geq 80°$) Sa–Sd host galaxies. He showed that the distribution can be well fitted by a sech^2 profile. However, these studies used only linear scales to estimate the vertical distribution of SNe. This is somewhat undesirable because the absolute distribution of SN heights (in kpc) is biased by the greatly different intrinsic sizes of host discs (as already shown in Fig. 3).

Most recently, Pavlyuk & Tsvetkov (2016) studied the absolute (in kpc) and relative (normalized to the radius of host galaxy) vertical distributions of SNe using a sample of 26 Type Ia, 8 Ibc and 44 II SNe in spiral host galaxies with $i \geq 85°$. They found that the distributions can be fitted by exp profiles with scale heights $\tilde{H}_{\text{Ia}} = 0.030 \pm 0.006$, $\tilde{H}_{\text{Ibc}} = 0.024 \pm 0.006$ and $\tilde{H}_{\text{II}} = 0.029 \pm 0.005$. The scale heights for Type Ibc and II SNe are in good agreement with our $\tilde{H}_{\text{CC}} = 0.028 \pm 0.003$ in Sa–Sd galaxies, while the scale height for Type Ia SNe is much smaller than our $\tilde{H}_{\text{Ia}} = 0.055 \pm 0.007$ in the same morphological bin. However, the direct comparison of the scale heights obtained by Pavlyuk & Tsvetkov (2016) with ours is difficult because they used the DSS images for the reduction of SNe host galaxies without mentioning the photometric band (we assume that they used *B*-band), while we use the SDSS *g*-band to normalize the heights to the 25th magnitude isophotal semimajor axes of host galaxies. On the other hand, we are not able to check the consistency between the morphological distributions of edge-on galaxies hosting Type Ia and CC SNe in their and our samples because morphological types were not provided by Pavlyuk & Tsvetkov (2016).

To exclude any dependence of scale height of the host stellar population on the morphological type, we analyse the vertical distribution of SNe in the most populated morphological bins, i.e. in the narrower Sb–Sc subsample (see Table 1).[11] In addition, the Sb–Sc subsample is more suitable for the comparison of the estimated vertical scale heights of SNe with those of different stellar

[11] On the other hand, by selecting these bins we reduce the possible contribution by SNe Ia from central bulges of host galaxies, although the bulge contribution is only up to 9 per cent of the total SN Ia population in Sa–Sd host galaxies (Barkhudaryan et al., in preparation).

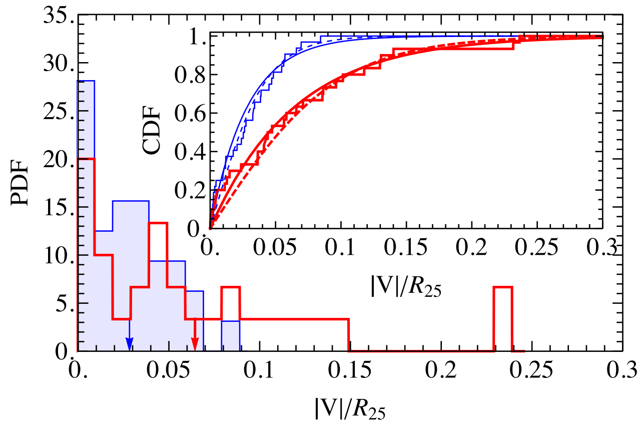

Figure 6. Vertical distributions of Type Ia (red thick line) and CC (blue thin line) SNe in Sb–Sc galaxies. The inset presents the cumulative distributions of SNe and fitted sech^2 (dashed curve) and exp (solid curve) CDFs. The mean values of the distributions are shown by arrows.

populations of thick and thin discs of the MW galaxy (see Section 4.2), and to exclude a small number of very thin discs (see e.g. Bizyaev et al. 2017), which usually appear in late-type galaxies.

From Table 2, we conclude that the vertical distributions of Type Ia and CC SNe in Sb–Sc galaxies can be well fitted by both the sech^2 and exp profiles. The vertical distribution of CC SNe is significantly different from that of Type Ia SNe (Table 3), being 2.3 ± 0.5 times more concentrated to the plane of the host disc (Table 2). This difference also exists when the above-mentioned effect of the dust extinction is considered for the particular subsample (Sb–Sc hosts labelled with '†' symbols in Tables 2 and 3). In Fig. 6, we present the comparison of vertical distributions as well as the fitted sech^2 and exp CDFs between both the types of SNe in Sb–Sc host galaxies.

It is important to note that Type Ia SNe, because of their comparatively high luminosity (in about two absolute magnitudes in *B*-band, e.g. Richardson et al. 2002) and the presence of dedicated surveys, are discovered at much greater distances than CC SNe (see Paper I). To check the possible distance biasing on the vertical distribution of SNe, we truncate the sample of Sb–Sc galaxies to

Table 4. Comparison of the $\tilde{H}_{\rm SN}$ values of Type Ia and CC SNe in edge-on Sb–Sc galaxies with those of the MW thick and thin discs.

Host	$\tilde{H}$	Reference
MW thin disc	0.020 ± 0.005	Jurić et al. (2008)
MW thin disc	0.022 ± 0.003	Chen et al. (2001)
MW thin disc	0.022 ± 0.005	Larsen & Humphreys (2003)
SNe CC (Sb–Sc)	$\mathbf{0.028 \pm 0.003}$	**This study**
MW thick disc	0.050 ± 0.005	Chen et al. (2001)
MW thick disc	0.051 ± 0.005	Robin et al. (1996)
MW thick disc	0.057 ± 0.014	Ojha (2001)
MW thick disc	0.058 ± 0.005	Larsen & Humphreys (2003)
MW thick disc	0.060 ± 0.013	Jurić et al. (2008)
MW thick disc	0.061 ± 0.020	Buser et al. (1999)
SNe Ia (Sb–Sc)	$\mathbf{0.065 \pm 0.012}$	**This study**
MW thick disc	0.067 ± 0.008	Ng et al. (1997)

Notes. The MW $\tilde{H}$ values are calculated using the original values of H from the references and assuming $R_{25}^{\rm MW} = 15 \pm 1$ kpc. The $\tilde{H}$ values are listed in the ascending order.

distances ≤200 Mpc.[12] In Table 2, the comparison of $\langle|\tilde{z}|\rangle$, $\tilde{z}_0^{\rm SN}$ and $\tilde{H}_{\rm SN}$ as well as $P_{\rm KS}$ and $P_{\rm AD}$ values of the distance-truncated sample (labelled with '*' symbols) with those of Sb–Sc host galaxies allows us to conclude that the possible distance biasing in our sample is negligible. Due to the smaller number statistics, we get larger error bars in Table 2 and lose only the KS test significance in Table 3. Therefore, in the remainder of this study, we will use SNe in Sb–Sc galaxies without distance-truncation.

4.2 The thick and thin discs

It is largely accepted that the disc of the MW, one of the well-studied representatives of Sb–Sc classes, is separated into at least three components/populations: (1) the youngest star-forming disc ($\tilde{H} \lesssim 0.01$), including molecular clouds and massive young stars (2) the younger thin disc ($\tilde{H} \sim 0.02$) that contains stars with a wide range of ages and (3) the old thick disc ($\tilde{H} \sim 0.06$), composed almost exclusively of older stars (Gilmore & Reid 1983; Robin et al. 1996; Ng et al. 1997; Buser, Rong & Karaali 1999; Chen et al. 2001; Ojha 2001; Chen, Hou & Wang 2003; Larsen & Humphreys 2003; Jurić et al. 2008; Bobylev & Bajkova 2016). For extragalactic discs of nearby edge-on spirals, the thick and thin components are also resolved (e.g. Seth et al. 2005; Yoachim & Dalcanton 2006). In this sense, we may be able to put constraints on the nature of the progenitors of Type Ia and CC SNe by comparing the parameters of their distributions ($\tilde{H}_{\rm SN}$ or $\tilde{z}_0^{\rm SN}$ and $h_{\rm SN}/z_0^{\rm SN}$ or $h_{\rm SN}/H_{\rm SN}$) in edge-on Sb–Sc galaxies with those of different stellar populations of thick and thin discs of MW and other similar galaxies. Note that the mean luminosity of our sample of Sb–Sc host galaxies ($\langle M_{\rm g}\rangle = -20.5 \pm 1.0$) is in good agreement with that of the MW ($\langle M_{\rm g}^{\rm MW}\rangle = -21.0 \pm 0.5$, Licquia, Newman & Brinchmann 2015).

In Table 4, we list the exp scale heights of SNe estimated in this study and the exp scale heights of the MW thick and thin discs derived from star counts (from hundreds of thousands to millions of

[12] It would be more effective to check this with distance-truncation at 150 (100) Mpc (see Papers II and III), however the remaining statistics in this case is very low, which destroys any comparison with significance. With the mentioned distance-truncation, we have only 19 (9) Type Ia SNe with $\langle|\tilde{z}|\rangle = 0.071 \pm 0.019$ (0.086 ± 0.025) and 30 (24) CC SNe with $\langle|\tilde{z}|\rangle = 0.027 \pm 0.005$ (0.031 ± 0.006).

Table 5. Comparison of the length/height ratios of Type Ia and CC SNe in Sb–Sc galaxies with those of the MW stars in the thick and thin discs.

Host	h/H	Reference
SNe Ia (Sb–Sc)	$\mathbf{3.08 \pm 0.65}$	**This study**
MW thick disc	3.30 ± 1.97	Buser et al. (1999)
MW thick disc	3.68 ± 1.08	Robin et al. (1996)
MW thick disc	4.00 ± 1.13	Jurić et al. (2008)
MW thick disc	4.30 ± 1.29	Ojha (2001)
MW thick disc	4.50 ± 0.46	Ng et al. (1997)
MW thick disc	5.41 ± 0.41	Larsen & Humphreys (2003)
MW thin disc	6.82 ± 3.03	Chen et al. (2001)
SNe CC (Sb–Sc)	$\mathbf{7.14 \pm 1.05}$	**This study**
MW thin disc	8.67 ± 2.45	Jurić et al. (2008)
MW thin disc	10.86 ± 2.70	Larsen & Humphreys (2003)

Notes. For both the types of SNe, we use $\tilde{h}_{\rm SN} = 0.20 \pm 0.02$ (Paper III). The h/H values are listed in the ascending order.

individual stars) by other authors. As can be seen, the scale height of the vertical distribution of CC SNe is consistent with those of younger stellar population in the thin disc (a wide range of ages up to a few Gyr; Loebman et al. 2011), while the scale height of Type Ia SNe is consistent with those of old population in the thick disc (from a few Gyr up to ∼10 Gyr; Loebman et al. 2011) of the MW galaxy.

Note that, in Table 4, the MW $\tilde{H}$ values are calculated using the original values of H (in kpc) from the references and assuming $R_{25}^{\rm MW} = 15 \pm 1$ kpc, i.e. $\tilde{H} = H/R_{25}^{\rm MW}$, while the ratio of radial to vertical scales (h/H) would be better for a comparison of SNe distribution with the distribution of stars in the MW, avoiding the use of an ambiguous value of $R_{25}^{\rm MW}$.

In Paper III, we studied the radial distributions of SNe and estimated the scale lengths of Type Ia and CC SNe using a well-defined sample of 500 nearby SNe and their low-inclined ($i \leq 60°$) and morphologically non-disturbed S0–Sm host galaxies from the SDSS.[13] In particular, the radial distributions of Type Ia and CC SNe in spiral galaxies are consistent with one another and with an exponential surface density according to $\exp(-\tilde{r}/\tilde{h}_{\rm SN})$ in Equation (3), where $\tilde{r} = R_{\rm SN}/R_{25}$ and $\tilde{h}_{\rm SN} = h_{\rm SN}/R_{25} = 0.21 \pm 0.02$. However, to be consistent with this study, we use the estimation of the scale lengths of SNe restricted to Sb–Sc host galaxies from that sample. Note that the similar determination of the sample of this paper is not possible because of its extreme inclination. For both types of SNe, we find $\tilde{h}_{\rm SN} = 0.20 \pm 0.02$ using 79 Type Ia and 198 CC SNe.

In Table 5, we list the ratios of radial to vertical scales of SNe ($h_{\rm SN}/H_{\rm SN}$) estimated in this study and the analogous ratios of MW thick and thin discs derived from star counts by other authors. The ratio of scales of CC SNe appears consistent with those of the younger stellar population in the thin disc, while the corresponding ratio of Type Ia SNe is consistent with the old population in the thick disc of the MW (although on the small side).

It should be noted that the parameters of the vertical distributions of different stellar populations in the MW are determined using samples dominated by stars relatively near the Sun, not including the sizable population of the disc (see the discussion in Bovy et al. 2012). Therefore, the structural parameters of the MW may be different from those of other galaxies. In particular, Seth

[13] At these inclinations, the dust extinction has minimal impact on the efficiency of SNe discovery (e.g. Cappellaro & Turatto 1997), making the estimation of the scale lengths as the most reliable.

Table 6. Comparison of the length to sech^2 height ratios of Type Ia and CC SNe in Sb–Sc galaxies with those detected from resolved stars in nearby edge-on galaxies and from unresolved populations of extragalactic thick and thin discs.

Host	h/z_0	Reference
Edge-on Sc galaxies^a (RGB-box)	1.83 ± 0.99	Seth et al. (2005)
SNe Ia (Sb–Sc)	$\mathbf{2.08 \pm 0.40}$	**This study**
Edge-on Sc galaxies^a (AGB-box)	2.40 ± 1.30	Seth et al. (2005)
Edge-on galaxies^b (thick+thin disc)	2.67 ± 0.86	Bizyaev et al. (2014)
Edge-on Sd galaxies^c (thick disc)	2.87 ± 0.72	Yoachim & Dalcanton (2006)
Edge-on Sc galaxies^a (MS-box)	3.83 ± 1.79	Seth et al. (2005)
SNe CC (Sb–Sc)	$\mathbf{4.76 \pm 0.93}$	**This study**
Edge-on Sd galaxies^c (thin disc)	5.48 ± 1.15	Yoachim & Dalcanton (2006)

Notes. For both the types of SNe, we use $\tilde{h}_{\rm SN} = 0.20 \pm 0.02$ (Paper III). The h/z_0 values are listed in the ascending order.
[a]The mean ratio of all six galaxies with the additional components of NGC 55 and NGC 4631 (from table 4 in Seth et al. 2005). These galaxies have lower masses than the MW.
[b]To be consistent with this study and the mentioned references, the mean ratio in *g*-band is estimated for a subsample of 529 galaxies from table 4 in Bizyaev et al. (2014) with a bulge-to-total luminosity ratio (*B*/*T*) in the *r*-band between 0.2 and 0.4 and distances $\leq$200 Mpc (a few galaxies, with obviously incorrect *B*/*T* values, are removed). The mean luminosity of this subsample ($\langle M_{\rm g} \rangle = -20.9 \pm 0.7$, corrected for Galactic extinction) is in good agreement with that of our Sb–Sc host galaxies ($\langle M_{\rm g} \rangle = -20.5 \pm 1.0$).
[c]The mean ratio of all 34 galaxies in *R*-band from table 4 in Yoachim & Dalcanton (2006). These galaxies have lower kinematic masses than the MW.

et al. (2005) analysed the vertical distribution of the resolved stellar populations in nearby six edge-on Sc galaxies observed with the *Hubble Space Telescope* and found that the ratios of radial to vertical scales of young star-forming discs are much smaller (∼3–4 times) than that of the MW. In other words, the young star-forming discs of their sample galaxies are much thicker in comparison with that of the MW. Their results are in agreement with those of Yoachim & Dalcanton (2006), who analysed the vertical structure of 34 late-type, edge-on, undisturbed disc galaxies using the two-dimensional fitting to their photometric profiles.

Interestingly, Seth et al. (2005) found that the scale height of a stellar population increases with age, which is also correct for the MW galaxy (e.g. Chen et al. 2003; Bovy et al. 2012). They used colour–magnitude diagrams (CMDs) to estimate the ages of resolved stellar populations (see figs 1 and 4 in Seth et al. 2005). The young population in their main-sequence (MS) box of the CMD is dominated by stars with ages from ∼10 up to ∼100 Myr; the intermediate population in the asymptotic giant branch (AGB) box is dominated by stars with ages from a few 100 Myr up to a few Gyr, while the old population in the red giant branch (RGB) box is dominated by stars with ages from a few Gyr up to ∼10 Gyr. In light of this, we compare in Table 6 the ratios of radial to vertical scales of SNe with those detected from resolved stars in nearby edge-on late-type galaxies (e.g. Seth et al. 2005) and from unresolved populations of extragalactic thick and thin discs estimated using the edge-on surface brightness profiles (e.g. Yoachim & Dalcanton 2006; Bizyaev et al. 2014).[14]

In Table 6, we see that the ratio of scales of the distribution of CC SNe is consistent with those of the resolved MS-box stars in Seth et al. (2005) and unresolved stellar population of the thin disc in Yoachim & Dalcanton (2006). On the other hand, the $h_{\rm SN}/z_0^{\rm SN}$ ratio of Type Ia SNe is consistent and located between the values of the same ratios of resolved RGB- and AGB-box stars, respectively (Seth et al. 2005). In addition, the $h_{\rm SN}/z_0^{\rm SN}$ ratio of Type Ia SNe is consistent with those of the unresolved population of the thick disc in Yoachim & Dalcanton (2006) and with the thick+thin disc population in Bizyaev et al. (2014).

These results are in good agreement with the age–scale height relation of stars in galaxy discs (e.g. Seth et al. 2005; Bovy et al. 2012), and that Type Ia SNe result from stars of different ages (from ∼0.5 up to ∼10 Gyr, see Maoz & Mannucci 2012), with even the shortest lifetime progenitors having much longer lifetime than the progenitors of CC SNe (from a few Myr up to ∼0.2 Gyr; see Zapartas et al. 2017).

5 CONCLUSIONS

In this fifth paper of a series, using a well-defined and homogeneous sample of SNe and their edge-on host galaxies from the coverage of SDSS DR12, we analyse the vertical distributions and estimate the sech^2 and exp scale heights of the different types of SNe, associating them to the thick or thin disc populations of galaxies. Our sample consists of 100 nearby (the mean distance is 100 ± 8 Mpc), high-inclination ($i \geq 85^\circ$) and morphologically non-disturbed S0–Sd galaxies, hosting 102 SNe in total.

The extinction by dust near to the plane of edge-on host galaxies has an insignificant impact on our estimated SN scale heights, although as was shown previously (e.g. Paper I), it is significantly decreasing the efficiency of SN discovery in these galaxies. We also check that there is no strong redshift bias within our SNe and host galaxies samples, which could drive the observed behaviours of the vertical distributions of the both SN types in host galaxies with edge-on discs.

The results obtained in this paper are summarized below, along with their interpretations.

(i) For the first time, we show that in both early- and late-type edge-on spiral galaxies the vertical distribution of CC SNe is about twice more concentrated to the plane of the host disc than the distribution of Type Ia SNe (Fig. 4 and Table 2). The difference

[14] Here, to be consistent with the original values from the references, we use the $h_{\rm SN}/z_0^{\rm SN}$ ratios.

between the distributions of the SN types is statistically significant with only the exception in late-type hosts (Table 3).

(ii) When considering early- and late-type spiral galaxies separately, the vertical distributions of Type Ia and CC SNe are consistent with both the sech^2 and exp profiles (Table 2). In wider morphological bins (S0–Sd or Sa–Sd), the vertical distribution of Type Ia SNe is not consistent with sech^2 profile, most probably due to the earlier and wider morphological distribution of SNe Ia host galaxies in comparison with CC SNe hosts (Table 1), and the systematically thinner vertical distribution of the host stellar population from early- to late-type discs.

(iii) By narrowing the host morphologies to the most populated Sb–Sc galaxies (close to the MW morphology) of our sample, we exclude the morphological biasing of host galaxies between the SN types and the dependence of the scale height of the host stellar population on the morphological type. In these galaxies, we find that the sech^2 scale heights ($\tilde{z}_0^{\rm SN}$) of Type Ia and CC SNe are 0.096 ± 0.016 and 0.042 ± 0.007, respectively. The exp scale heights ($\tilde{H}_{\rm SN}$) are 0.065 ± 0.012 and 0.028 ± 0.003, respectively. In Sb–Sc galaxies, the vertical distribution of CC SNe is significantly different from that of Type Ia SNe (Table 3), being 2.3 ± 0.5 times more concentrated to the plane of the host disc (Table 2).

(iv) In Sb–Sc hosts, the exp scale height (also the $h_{\rm SN}/H_{\rm SN}$ ratio) of CC SNe is consistent with that of the younger stellar population in the thin disc of the MW, derived from star counts, while the scale height (also the ratio) of SNe Ia is consistent with that of the old population in the thick disc of the MW (Tables 4 and 5).

(v) For the first time, we show that the ratio of scale lengths to scale heights ($h_{\rm SN}/z_0^{\rm SN}$) of the distribution of CC SNe is consistent with those of the resolved young stars with ages from ∼10 up to ∼100 Myr in nearby edge-on galaxies and the unresolved stellar population of extragalactic thin discs (Table 6). On the other hand, the corresponding ratio for Type Ia SNe is consistent and located between the values of the same ratios of the two populations of resolved stars with ages from a few 100 Myr up to a few Gyr and from a few Gyr up to ∼10 Gyr, as well as with the unresolved population of the thick disc of nearby edge-on galaxies.

All these results can be explained considering the age–scale height relation of the distribution of the stellar population and the mean age difference between Type Ia and CC SNe progenitors.

ACKNOWLEDGEMENTS

We would like to thank the anonymous referee for his/her commentary and also Massimo Della Valle for his constructive comments on the earlier drafts of this manuscript. AAH, LVB and AGK acknowledge the hospitality of the Institut d'Astrophysique de Paris (France) during their stay as visiting scientists supported by the Programme Visiteurs Extérieurs (PVE). This work was supported by the RA MES State Committee of Science, in the frames of the research project number 15T–1C129. AAH is also partially supported by the ICTP. VA acknowledges the support from Fundação para a Ciência e Tecnologia (FCT) through national funds and from FEDER through COMPETE2020 by the grants UID/FIS/04434/2013 and POCI-01-0145-FEDER-007672, and the support from FCT through Investigador FCT contract IF/00650/2015/CP1273/CT0001. This work was made possible in part by a research grant from the Armenian National Science and Education Fund (ANSEF) based in New York, USA. Funding for SDSS-III has been provided by the Alfred P. Sloan Foundation, the Participating Institutions, the National Science Foundation and the US Department of Energy Office of Science. The SDSS–III website is http://www.sdss3.org/. SDSS–III is managed by the Astrophysical Research Consortium for the Participating Institutions of the SDSS–III Collaboration including the University of Arizona, the Brazilian Participation Group, Brookhaven National Laboratory, University of Cambridge, University of Florida, the French Participation Group, the German Participation Group, the Instituto de Astrofisica de Canarias, the Michigan State/Notre Dame/JINA Participation Group, Johns Hopkins University, Lawrence Berkeley National Laboratory, Max Planck Institute for Astrophysics, New Mexico State University, New York University, Ohio State University, Pennsylvania State University, University of Portsmouth, Princeton University, the Spanish Participation Group, University of Tokyo, University of Utah, Vanderbilt University, University of Virginia, University of Washington and Yale University.

REFERENCES

Alam S. et al., 2015, ApJS, 219, 12
Anderson J. P., James P. A., 2008, MNRAS, 390, 1527
Anderson J. P., Habergham S. M., James P. A., Hamuy M., 2012, MNRAS, 424, 1372
Anderson J. P., James P. A., Habergham S. M., Galbany L., Kuncarayakti H., 2015, PASA, 32, e019
Andreasyan H. R., Andreasyan R. R., Paronyan G. M., 2016, Astrophysics, 59, 57
Aramyan L. S. et al., 2016, MNRAS, 459, 3130
Barbon R., Buondí V., Cappellaro E., Turatto M., 1999, A&AS, 139, 531
Bianchi S., 2007, A&A, 471, 765
Bizyaev D., Mitronova S., 2002, A&A, 389, 795
Bizyaev D. V., Kautsch S. J., Mosenkov A. V., Reshetnikov V. P., Sotnikova N. Y., Yablokova N. V., Hillyer R. W., 2014, ApJ, 787, 24
Bizyaev D. V., Kautsch S. J., Sotnikova N. Y., Reshetnikov V. P., Mosenkov A. V., 2017, MNRAS, 465, 3784
Bobylev V. V., Bajkova A. T., 2016, Astron. Lett., 42, 1
Bovy J., Rix H.-W., Liu C., Hogg D. W., Beers T. C., Lee Y. S., 2012, ApJ, 753, 148
Buser R., Rong J., Karaali S., 1999, A&A, 348, 98
Cappellaro E., Turatto M., 1997, in Ruiz-Lapuente P., Canal R., Isern J., eds, NATO Adv. Sci. Inst. Ser. C Vol. 486, Thermonuclear Supernovae. Springer-Verlag, Dordrecht, p. 77
Chen B. et al., 2001, ApJ, 553, 184
Chen L., Hou J. L., Wang J. J., 2003, AJ, 125, 1397
D'Agostino R. B., Stephens M. A., 1986, Goodness-of-fit Techniques, Statistics: Textbooks and Monographs, Vol. 68, Marcel Dekker, New York
Dawson P. C., Johnson R. G., 1994, J. Roy. Astron. Soc. Can., 88, 369
De Geyter G., Baes M., Camps P., Fritz J., De Looze I., Hughes T. M., Viaene S., Gentile G., 2014, MNRAS, 441, 869
de Grijs R., 1998, MNRAS, 299, 595
de Grijs R., Peletier R. F., 1997, A&A, 320, L21
de Grijs R., Peletier R. F., van der Kruit P. C., 1997, A&A, 327, 966
Della Valle M., Panagia N., 1992, AJ, 104, 696
Engmann S., Cousineau D., 2011, J. Appl. Quant. Methods, 6, 1
Filippenko A. V., 1997, ARA&A, 35, 309
Förster F., Schawinski K., 2008, MNRAS, 388, L74
Galbany L. et al., 2014, A&A, 572, A38
Galbany L. et al., 2016, A&A, 591, A48
Gilmore G., Reid N., 1983, MNRAS, 202, 1025
Habergham S. M., Anderson J. P., James P. A., Lyman J. D., 2014, MNRAS, 441, 2230
Hakobyan A. A., 2008, Astrophysics, 51, 69
Hakobyan A. A., Petrosian A. R., McLean B., Kunth D., Allen R. J., Turatto M., Barbon R., 2008, A&A, 488, 523
Hakobyan A. A., Mamon G. A., Petrosian A. R., Kunth D., Turatto M., 2009, A&A, 508, 1259

Hakobyan A. A., Adibekyan V. Z., Aramyan L. S., Petrosian A. R., Gomes J. M., Mamon G. A., Kunth D., Turatto M., 2012, A&A, 544, A81 (Paper I)
Hakobyan A. A. et al., 2014, MNRAS, 444, 2428 (Paper II)
Hakobyan A. A. et al., 2016, MNRAS, 456, 2848 (Paper III)
Hatano K., Branch D., Fisher A., Starrfield S., 1997a, MNRAS, 290, 113
Hatano K., Fisher A., Branch D., 1997b, MNRAS, 290, 360
Hatano K., Branch D., Deaton J., 1998, ApJ, 502, 177
Holwerda B. W., Reynolds A., Smith M., Kraan-Korteweg R. C., 2015, MNRAS, 446, 3768
Ilovaisky S. A., Lequeux J., 1972, A&A, 18, 169
Ivanov V. D., Hamuy M., Pinto P. A., 2000, ApJ, 542, 588
Jurić M. et al., 2008, ApJ, 673, 864
Kangas T. et al., 2017, A&A, 597, A92
Kelly P. L., Kirshner R. P., 2012, ApJ, 759, 107
Larsen J. A., Humphreys R. M., 2003, AJ, 125, 1958
Licquia T. C., Newman J. A., Brinchmann J., 2015, ApJ, 809, 96
Loebman S. R., Roškar R., Debattista V. P., Ivezić Ž., Quinn T. R., Wadsley J., 2011, ApJ, 737, 8
McMillan R. J., 1997, PhD thesis, Pennsylvania State University
McMillan R. J., Ciardullo R., 1996, ApJ, 473, 707
Maoz D., Mannucci F., 2012, PASA, 29, 447
Maoz D., Mannucci F., Nelemans G., 2014, ARA&A, 52, 107
Massey F. J., 1951, J. Am. Stat. Assoc., 46, 68
Modjaz M., Kewley L., Bloom J. S., Filippenko A. V., Perley D., Silverman J. M., 2011, ApJ, 731, L4
Molloy M., 2012, Master's thesis, Dublin City University
Mosenkov A. V., Sotnikova N. Y., Reshetnikov V. P., 2010, MNRAS, 401, 559
Nazaryan T. A., Petrosian A. R., Hakobyan A. A., Adibekyan V. Z., Kunth D., Mamon G. A., Turatto M., Aramyan L. S., 2013, Ap&SS, 347, 365
Ng Y. K., Bertelli G., Chiosi C., Bressan A., 1997, A&A, 324, 65
Ojha D. K., 2001, MNRAS, 322, 426
Paturel G. et al., 1997, A&AS, 124
Pavlyuk N. N., Tsvetkov D. Y., 2016, Astron. Lett., 42, 495
Perets H. B. et al., 2010, Nature, 465, 322
Petrosian A. et al., 2005, AJ, 129, 1369
Pettitt A. N., 1976, Biometrika, 63, 161
Reshetnikov V. P., Mosenkov A. V., Moiseev A. V., Kotov S. S., Savchenko S. S., 2016, MNRAS, 461, 4233
Richardson D., Branch D., Casebeer D., Millard J., Thomas R. C., Baron E., 2002, AJ, 123, 745
Robin A. C., Haywood M., Creze M., Ojha D. K., Bienayme O., 1996, A&A, 305, 125
Seth A. C., Dalcanton J. J., de Jong R. S., 2005, AJ, 130, 1574
Smartt S. J., 2009, ARA&A, 47, 63
Smith N., Li W., Filippenko A. V., Chornock R., 2011, MNRAS, 412, 1522
Spergel D. N. et al., 2007, ApJS, 170, 377
Spitzer L., Jr, 1942, ApJ, 95, 329
Taddia F. et al., 2015, A&A, 580, A131
Tsvetkov D. Y., 1981, Sov. Astron. Lett., 7, 254
Tsvetkov D. Y., 1987, Sov. Astron., 31, 39
Turatto M., 2003, in Weiler K., ed., Lecture Notes in Physics, Vol. 598, Supernovae and Gamma-Ray Bursters. Springer-Verlag, Berlin, p. 21
van den Bergh S., 1997, AJ, 113, 197
Wang X., Wang L., Filippenko A. V., Zhang T., Zhao X., 2013, Science, 340, 170
Yoachim P., Dalcanton J. J., 2006, AJ, 131, 226
Zapartas E. et al., 2017, A&A, 601, A29

SUPPORTING INFORMATION

Supplementary data are available at *MNRAS* online

PaperVonlinedata.csv

Please note: Oxford University Press is not responsible for the content or functionality of any supporting materials supplied by the authors. Any queries (other than missing material) should be directed to the corresponding author for the article.

This paper has been typeset from a TEX/LATEX file prepared by the author.